AIAA JOURNAL
Vol. 33, No. 12, December 1995

Buckling of Rectangular Symmetric Angle-Ply Laminated Plates Determined by Eigensensitivity Analysis

O. Barton Jr.*
U.S. Naval Academy, Annapolis, Maryland 21402
and
R. Reiss†
Howard University, Washington, D.C. 20056

Closed-form approximate solutions for uniaxial and biaxial compressive buckling of rectangular symmetric angle-ply laminates are developed from eigensensitivity analysis. Boundary conditions, which consist of the various combinations of clamped and simply supported edges, are incorporated through appropriate edge condition parameters. Calculated results, presented for elastic moduli ratios up to 40, compare quite favorably with the corresponding buckling loads obtained from the Ritz method.

Nomenclature

a, b	= dimension of rectangular plate in x and y directions
$\hat{a}_{mn}$	= eigenvector
C_{ij}, G_{ij}, H_{ij}	= matrices defining the boundary conditions where x is defined as constant
c_{ij}, g_{ij}, h_{ij}	= matrices defining the boundary conditions where y is defined as constant
D_{ij}	= bending stiffnesses of composite laminate
e_{mn}	= unit vector whose only nonzero component is the (m, n)th component
E, M	= self adjoint operators
$[K], [M]$	= symmetric matrices equivalent to E, M operators, respectively
K_{pqmn}, M_{pqmn}	= elements of the $[K]$ and $[M]$ matrices
$[K_D], [M_D]$	= diagonal matrices obtained by setting the off-diagonal elements of $[K]$ and $[M]$ equal to zero
$[\Delta K], [\Delta M]$	= zero-diagonal matrices obtained by setting the diagonal elements of $[K]$ and $[M]$ equal to zero
$\hat{k}_i, k_i$	= normalized Ritz critical buckling load
k_{ij}	= normalized approximate buckling load
N_x, N_y	= in-plane stress resultants
Q	= transformation matrix
R	= plate's aspect ratio a/b
S_1, S_2	= dummy parameters
T, T^*	= mutually adjoint differential operators
$X_m(x/a), Y_n(y/b)$	= normalized beam shape functions on (0,1)
U_{ij}	= eigenfunction
U_1	= invariant material property
w	= transverse deflection
α_{ijmn}	= (m, n)th component of the eigenvector α_{ij}
β	= ratio of in-plane stress resultants N_y/N_x
θ	= laminate ply angle with respect to the x axis
λ_{ij}	= eigenvalue corresponding to eigenfunction U_{ij}
μ_p, ν_q	= beam's frequencies corresponding to X_p and Y_q
ψ_{mn}	= basis functions
Ω	= domain of plate

Presented as Paper 94-1574 at the AIAA/ASME/ASCE/AHS/ASC 35th Structures, Structural Dynamics, and Materials Conference, Hilton Head, SC, April 18–20, 1994; received July 22, 1994; revision received March 10, 1995; accepted for publication March 13, 1995.

*Assistant Professor, Mechanical Engineering Department. Member AIAA.
†Professor, Department of Mechanical Engineering. Member AIAA.

Background

ONE of the earliest buckling analysis of anisotropic plates was performed by Chamis[1] who examined the stability of simply supported anisotropic plates subject to a combination of edge loads. He employed a Galerkin procedure to discretize the system and computed the buckling load using the power method. Ashton and Whitney[2] obtain the critical buckling load for uniaxially compressed simply supported symmetric angle-ply laminates. Beam shape functions are employed in a Rayleigh–Ritz approach to obtain an approximate solution. Tauchert[3] uses a Reissner–Mindlin theory to estimate the thermal buckling loads for moderately thick antisymmetric angle-ply laminates. Pandey and Sherbourne[4] employ orthogonal polynomials as basis functions in a Ritz scheme. Critical buckling load are determined by Tang and Sridharan[5] from perturbation theory.

Finite element solutions also appear to be quite popular. Chang and Chiu,[6] Lin and Kuo,[7] Teply et al.,[8] and Chen and Yang[9] are just some of the investigators who employ finite element or hybrid finite element models to solve specific classes of laminated plates and/or edge conditions.

Exact or approximate closed-form solutions for the stability of laminated plates are scarce. Although numerically based solutions can be obtained for many problems, there are obvious advantages for closed-form solutions, albeit approximate. The foremost among these advantages occurs in design optimization, where repeated and often costly analysis is eliminated if the solution is available in closed form.

Khdeir[10] treats buckling of symmetric cross-ply rectangular laminates with one pair of opposite edges simply supported. He employs a Levy type solution in conjunction with a state space formulation to numerically determine the exact buckling loads. To the authors' knowledge exact closed-form solutions are limited to specially orthotropic simply supported plates,[11] antisymmetric cross-ply laminates satisfying the S2 boundary condition,[12] and antisymmetric angle-plies obeying the S3 boundary condition.[13] By using eigensensitivity analysis, Reiss and Barton[14] developed approximate expressions for the buckling loads of simply supported rectangular symmetric angle-ply laminates by expanding the buckling load in a Fourier series in the ply angle θ.

In the present paper, the objective is to develop an expression which can be used to compute the critical buckling load of symmetric angle-ply composite laminates obeying combinations of simply supported and clamped boundary conditions. Beam shape functions for the Ritz method in conjunction with eigensensitivity techniques will be used to determine approximate formulas for the eigenvalues.

Problem Statement

The governing equation for biaxial buckling of composite symmetric laminates[11] is given by

$$D_{11}\frac{\partial^4 w}{\partial x^4}+4D_{16}\frac{\partial^4 w}{\partial x^3\partial y}+2(D_{12}+2D_{66})\frac{\partial^4 w}{\partial x^2\partial y^2}$$

$$+4D_{26}\frac{\partial^4 w}{\partial x\partial y^3}+D_{22}\frac{\partial^4 w}{\partial y^4}=N_x\left(\frac{\partial^2 w}{\partial x^2}+\beta\frac{\partial^2 w}{\partial y^2}\right) \tag{1}$$

For uniaxial buckling in the x direction $\beta = 0$ and for equal biaxial compression $\beta = 1$. For uniaxial buckling in the y direction, the x and y directions may be interchanged to obtain $\beta = 0$. Each edge of the rectangular laminate is either clamped or simply supported. It is desired to obtain a closed-form approximation for N_x in terms of the D_{ij}, β, the plate's aspect ratio R, and boundary condition parameters.

Eigensensitivity Analysis

Preliminaries

Consider the abstract eigenvalue problem defined by

$$T^*E(S)TU_{ij}=\lambda_{ij}M(S)U_{ij} \tag{2}$$

in the domain Ω. The double indices are used to facilitate a separable eigenfunction expansion later. Appropriate boundary conditions must be appended to Eq. (2) for a well-posed problem. When M is an appropriate differential operator, Eq. (2) describes stability.

It is first necessary to determine a discrete form equivalent to Eq. (2). Toward this end, select a kinematically admissible, complete, and linearly independent basis sequence $\{\psi_{mn}\}$ spanning the domain of kinematically admissible functions. Therefore, the eigenfunction can be approximated by

$$U_{ij}=\sum_{m=0}^{N}\sum_{n=0}^{N}\alpha_{ijmn}\psi_{mn} \tag{3}$$

where Eq. (3) becomes exact as $N\to\infty$.

The discretized Ritz equations. corresponding to Eq. (2) are

$$\sum_m\sum_n K_{pqmn}\alpha_{ijmn}=\lambda_{ij}\sum_m\sum_n M_{pqmn}\alpha_{ijmn} \tag{4}$$

where

$$K_{pqmn}=(T\psi_{pq},ET\psi_{mn}),\qquad M_{pqmn}=(\psi_{pq},M\psi_{mn}) \tag{5}$$

and $(\cdot,\cdot)$ denotes the $L_2(\Omega)$ inner product. Equation (4), when expressed in matrix form, becomes

$$[K]\{\alpha_{ij}\}=\lambda_{ij}[M]\{\alpha_{ij}\} \tag{6}$$

Equation (6) has N^2 degrees of freedom. The discrete equation (6) is equivalent to the distributed parameter form (1) for sufficiently large N. If the required value of N is large enough, then Eq. (6) can become numerically intractable. Clearly, it is of interest to develop a method to determine λ_{ij} of Eq. (6) without directly solving the eigenvalue problem.

Approximate Eigenvalue Solution

Consider the equation

$$[\hat K(S_1)]\{\hat\alpha_{mn}(S_1,S_2)\}=\hat\lambda_{mn}(S_1,S_2)[\hat M(S_2)]\{\hat\alpha_{mn}(S_1,S_2)\} \tag{7}$$

where

$$[\hat K(S_1)]=[K_D]+S_1[\Delta K]\qquad [\hat M(S_2)]=[M_D]+S_2[\Delta M] \tag{8}$$

Here S_1 and S_2 are parameters which range from 0 to 1. If $S_1 = S_2 = 0$, the solution to Eq. (8) is trivial and if $S_1 = S_2 = 1$, the solution to Eq. (7) coincides with the solution of Eq. (6).

An approximate solution for Eq. (6) can be developed by expressing the solution $\hat\lambda_{mn}(S_1, S_2)$ as a Maclaurin series in S_1, S_2 and evaluating result at $S_1 = S_2 = 1$. Thus,

$$\lambda_{mn}=\hat\lambda_{mn}(1,1)\cong\hat\lambda_{mn}(0,0)+\delta\hat\lambda_{mn}(0,0)+\tfrac{1}{2}\delta^2\hat\lambda_{mn}(0,0) \tag{9}$$

where

$$\hat\lambda_{mn}(0,0)=K_{mnmn}/M_{mnmn} \tag{10}$$

and the corresponding eigenvector is

$$\hat\alpha_{mn}(0,0)=e_{mn}\big/\sqrt{M_{mnmn}} \tag{11}$$

Calculation of the remaining terms on the right-hand side of Eq. (9) is a bit more involved. Toward this end, observe that

$$\{\hat\alpha_{mn}\}=\hat\lambda_{mn}[\hat K]^{-1}[\hat M]\{\hat\alpha_{mn}\} \tag{12}$$

By taking the first variation of Eq. (12), gathering like terms in $\delta\{\hat\alpha_{mn}\}$, and premultiplying by $[\hat K]$ one obtains

$$[\hat K]\delta\{\hat\alpha_{mn}\}-\hat\lambda_{mn}[\hat M]\delta\{\hat\alpha_{mn}\}=\delta\hat\lambda_{mn}[\hat M]\{\hat\alpha_{mn}\}$$

$$+\hat\lambda_{mn}[\hat K]\delta([\hat K]^{-1})[\hat M]\{\hat\alpha_{mn}\}+\hat\lambda_{mn}\delta[\hat M]\{\hat\alpha_{mn}\}\equiv\{\hat F_{mn}\} \tag{13}$$

Note that if $\{\hat F_{mn}\}\equiv\{0\}$, Eq. (7) shows that the solution to Eq. (13) would be $\delta\{\hat a_{mn}\}=\{\hat a_{mn}\}$. A theorem[15] from linear algebra states a necessary condition for the existence of a solution to Eq. (13) is that $\{\hat F_{mn}\}$ is orthogonal to every solution of Eq. (7), that is,

$$\{\hat a_{mn}\}^T\{\hat F_{mn}\}=0 \tag{14}$$

Substitution of Eq. (13) into Eq. (14) yields

$$\delta\hat\lambda_{mn}\{\hat a_{mn}\}^T[\hat M]\{\hat a_{mn}\}+\hat\lambda_{mn}\{\hat a_{mn}\}^T[\hat K][\delta\hat K]^{-1}[\hat M]\{\hat a_{mn}\}$$

$$+\hat\lambda_{mn}\{\hat a_{mn}\}^T[\delta\hat M]\{\hat a_{mn}\}=0 \tag{15}$$

By observing that $\delta K = \Delta K$ and $\delta M = \Delta M$ and using Eq. (12), the solution for $\delta\hat\lambda_{mn}$ becomes

$$\delta\hat\lambda_{mn}=\frac{\{\hat a_{mn}\}^T[\Delta K]\{\hat a_{mn}\}-\hat\lambda_{mn}\{\hat a_{mn}\}^T[\Delta M]\{\hat a_{mn}\}}{\{\hat a_{mn}\}^T[\hat M]\{\hat a_{mn}\}} \tag{16}$$

By evaluating Eq. (16) at $S_1 = S_2 = 0$, it follows that

$$\delta\hat\lambda_{mn}(0,0)=0 \tag{17}$$

It now remains to determine $\delta^2\hat\lambda_{mn}$. For simplicity, suppose the eigenvectors $\{\hat a_{mn}\}$ are normalized with respect to $[\hat M]$. Then take the variation of Eq. (16) to determine

$$\delta^2\hat\lambda_{mn}=2\delta\{\hat\alpha_{mn}\}^T[\Delta K]\{\hat\alpha_{mn}\}-2\hat\lambda_{mn}\delta\{\hat\alpha_{mn}\}^T[\Delta M]\{\hat\alpha_{mn}\}$$

$$-\delta\hat\lambda_{mn}\{\hat\alpha_{mn}\}^T[\Delta M]\{\hat\alpha_{mn}\} \tag{18}$$

All expressions required for $\delta^2\hat\lambda_{mn}$ are known except for $\delta\{\hat\alpha_{mn}\}$. To compute $\delta\{\hat\alpha_{mn}\}$, expand it in the form

$$\delta\{\hat\alpha_{mn}\}=\sum_p\sum_q\hat A_{mnpq}\{\hat\alpha_{pq}\} \tag{19}$$

Here $\hat A_{mnpq}$ are functions of S_1 and S_2. The problem of determining $\delta\{\hat\alpha_{mn}\}$ has been reduced to determining the coefficients $\hat A_{mnpq}$. This expansion closely follows the work of Reiss[16] who determined the eigenderivatives of self-adjoint distributed parameter eigenvalue problems. The first variation of Eq. (7) is

$$[\hat K]\delta\{\hat a_{mn}\}-\hat\lambda_{mn}[\hat M]\delta\{\hat a_{mn}\}=\delta\hat\lambda_{mn}[\hat M]\{\hat a_{mn}\}$$

$$-[\Delta K]\{\hat a_{mn}\}+\hat\lambda_{mn}[\Delta M]\{\hat a_{mn}\} \tag{20}$$

Now substitute Eq. (19) into Eq. (20), premultiply both sides of the resulting equation with $\{e_{rs}\}$, and set $S_1 = S_2 = 0$, to obtain

$$\hat A_{mnrs}(0,0)=\frac{K_{mnmn}\Delta M_{rsmn}-M_{mnmn}\Delta K_{rsmn}}{K_{rsrs}M_{mnmn}-K_{mnmn}M_{rsrs}}\times\frac{\sqrt{M_{rsrs}}}{\sqrt{M_{mnmn}}} \tag{21}$$

provided $(m,n)/(r,s)$ identically. Equations (19) and (21) can be combined to yield

$$\delta\{\hat{\alpha}_{mn}(0,0)\} = \frac{\hat{A}_{mnmn}(0,0)\{e_{mn}\}}{\sqrt{M_{mnmn}}} + \frac{1}{M_{mnmn}} \times \sum_r \sum_s \frac{K_{mnmn}\Delta M_{rsmn} - M_{mnmn}\Delta K_{rsmn}}{K_{rsrs}M_{mnmn} - K_{mnmn}M_{rsrs}} \times \{e_{rs}\} \tag{22}$$

Now, substitute Eq. (22) into Eq. (18) evaluated at (0,0), to obtain

$$\delta^2\hat{\lambda}_{mn}(0,0) = -\frac{2}{M^2_{mnmn}} \times \sum_{p\neq m}\sum_{q\neq n}\left\{\frac{[K_{mnmn}\Delta M_{pqmn} - M_{mnmn}\Delta K_{pqmn}]^2}{K_{pqpq}M_{mnmn} - K_{mnmn}M_{pqpq}}\right\} \tag{23}$$

$$A, B = \frac{M_{IJIJ}K_{PQPQ} + M_{PQPQ}K_{IJIJ}}{2M_{IJIJ}M_{PQPQ}} \mp \frac{\sqrt{(M_{IJIJ}K_{PQPQ} + K_{IJIJ}M_{PQPQ})^2 - 4M_{IJIJ}M_{PQPQ}(K_{IJIJ}K_{PQPQ} - K^2_{IJPQ})}}{2M_{IJIJ}M_{PQPQ}} \tag{29}$$

In Eq. (23), it is understood that (p,q) cannot be identically equal to (m,n). Finally, combining Eqs. (9), (10), (17), and (23) provides an approximate closed-form quadratic expression for the eigenvalue as

$$\lambda_{mn} = \frac{K_{mnmn}}{M_{mnmn}} - \frac{1}{M^2_{mnmn}} \times \sum_{p\neq m}\sum_{q\neq n}\left\{\frac{[K_{mnmn}\Delta M_{pqmn} - M_{mnmn}\Delta K_{pqmn}]^2}{K_{pqpq}M_{mnmn} - K_{mnmn}M_{pqpq}}\right\} \tag{24}$$

Furthermore, the solution (24) is exact to within cubic terms of the ΔK and ΔM elements provided the zeroth-order approximate eigenvalue $\hat{\lambda}_{mn}(0,0)$ [Eq. (10)] is not repeated. Higher order terms if needed may be derived in a similar manner.

Repeated Eigenvalues

It is well known that repeated eigenvalues cannot be differentiated.[16] In the previous section, the derivatives of the eigenvalues $\hat{\lambda}_{ij}(S_1,S_2)$ were evaluated at $S_1 = S_2 = 0$ in order to obtain the approximate series (9). However, if for some distinct pair of indices (I,J) and (P,Q)

$$K_{IJIJ}/M_{IJIJ} = K_{PQPQ}/M_{PQPQ} \tag{25}$$

so that $\hat{\lambda}_{IJ}(0,0) = \hat{\lambda}_{PQ}(0,0)$, then evaluation of Eq. (23) implies that $\delta^2\hat{\lambda}_{IJ}(0,0) = \infty$. Thus $\hat{\lambda}_{IJ}(0,0)$ is not differentiable at (0,0) and, consequently, the series expansion (9) is meaningless. Further, if Eq. (25) is approximately satisfied for these distinct pairs of indices, then $\hat{\lambda}_{IJ}$ can be $\hat{\lambda}_{PQ}$ differentiated at (0, 0), but their second derivatives are so large that the approximation (9), which only includes terms up to the second derivatives, cannot be justified. To circumvent this difficulty, observe that original matrices $[K]$ and $[M]$ may undergo similarity transformations without changing the eigenvalues. For simplicity, assume $[M]$ is diagonal. The values of the elements in the submatrices

$$\begin{bmatrix} K_{IJIJ} & K_{IJPQ} \\ K_{PQIJ} & K_{PQPQ}\end{bmatrix} \quad\text{and}\quad \begin{bmatrix} M_{IJIJ} & 0 \\ 0 & M_{PQPQ}\end{bmatrix} \tag{26}$$

are responsible for the singularities in $\hat{\lambda}_{IJ}$ and $\hat{\lambda}_{PQ}$. Therefore, let $[Q]$ simultaneously diagonalize both matrices (26). The new transformed matrices $[K']$ and $[M']$ satisfy

$$[K'] = [Q]^T[K][Q] \qquad [M'] = [Q]^T[M][Q] \tag{27}$$

where

$$\begin{aligned} Q_{IJIJ} &= \frac{K_{IJPQ}}{\sqrt{M_{IJIJ}K^2_{IJPQ} + M_{PQPQ}(K_{IJIJ} - AM_{IJIJ})^2}} \\ Q_{PQIJ} &= \frac{AM_{IJIJ} - K_{IJIJ}}{\sqrt{M_{IJIJ}K^2_{IJPQ} + M_{PQPQ}(K_{IJIJ} - AM_{IJIJ})^2}} \\ Q_{IJPQ} &= \frac{K_{IJPQ}}{\sqrt{M_{IJIJ}K^2_{IJPQ} + M_{PQPQ}(K_{IJIJ} - BM_{IJIJ})^2}} \\ Q_{PQPQ} &= \frac{BM_{IJIJ} - K_{IJIJ}}{\sqrt{M_{IJIJ}K^2_{IJPQ} + M_{PQPQ}(K_{IJIJ} - BM_{IJIJ})^2}} \end{aligned} \tag{28}$$

and

For all other indices

$$Q_{ijmn} = \delta_{im}\delta_{jn} \tag{30}$$

According to Eq. (27)

$$\begin{aligned} K'_{ijmn} &= \sum_r\sum_s\sum_p\sum_q K_{rspq}Q_{pqmn}Q_{rsij} \\ M'_{ijmn} &= \sum_r\sum_s\sum_p\sum_q M_{rspq}Q_{pqmn}Q_{rsij} \end{aligned} \tag{31}$$

Upon substituting Eqs. (28–30) into Eqs. (31), the elements of the transformed matrices become

$$\begin{gathered} K'_{IJIJ} = A \qquad K'_{PQPQ} = B \\ K'_{IJPQ} = K'_{PQIJ} = 0 \\ M'_{IJIJ} = M'_{PQPQ} = 1 \end{gathered} \tag{32}$$

$$\begin{gathered} K'_{IJmn} = Q_{IJIJ}K_{IJmn} + Q_{PQIJ}K_{PQmn} \\ K'_{PQmn} = Q_{IJPQ}K_{IJmn} + Q_{PQPQ}K_{PQmn} \\ M'_{mnmn} = M_{mnmn} \end{gathered} \tag{33}$$

where (m,n) range over all pairs of indices other than (I,J) and (P,Q). With Eqs. (32) and (33) the appropriate expressions for λ_{IJ} and λ_{PQ}, according to Eq. (25), are

$$\begin{aligned} \lambda_{IJ} &= A - \sum_m\sum_n \frac{(Q_{IJIJ}K_{IJmn} + Q_{PQIJ}K_{PQmn})^2}{K_{mnmn} - AM_{mnmn}} \\ \lambda_{PQ} &= B - \sum_m\sum_n \frac{(Q_{IJPQ}K_{IJmn} + Q_{PQPQ}K_{PQmn})^2}{K_{mnmn} - BM_{mnmn}} \end{aligned} \tag{34}$$

Equations (34) must be used to approximate λ_{IJ} and λ_{PQ} whenever Eq. (25) is satisfied. Also, they should be used whenever Eq. (25) is approximately satisfied. The other eigenvalues λ_{ij} may be evaluated from Eq. (24).

Finally, it should be pointed out that for the special case in which $K_{IJPQ} = 0$, Eq. (31) will still be satisfied for the transformed elements. Consequently, the $[Q]$ of Eqs. (28) and (30) accomplishes nothing. However, in this case, a different but equally simple transformation will accomplish the same objective.

Application to Stability Analysis of Symmetric Laminated Plates

To apply Eq. (24) to laminated plates, it is first necessary to cast Eq. (1) in the general form (2). This is accomplished by identifying

$$T^T = T^* = \left[\frac{\partial^2}{\partial x^2}\;\frac{\partial^2}{\partial y^2}\;\frac{2\partial^2}{\partial x\partial y}\right] \tag{35}$$

$$E = \begin{bmatrix} D_{11} & D_{12} & D_{16} \\ D_{12} & D_{22} & D_{26} \\ D_{16} & D_{26} & D_{66} \end{bmatrix} \tag{36}$$

$$M = \left(\frac{\partial^2}{\partial x^2} + \beta\frac{\partial^2}{\partial y^2}\right)$$

$$\lambda_{mn} = N_x \qquad \beta = N_y/N_x \tag{37}$$

The basis functions $\{\psi_{mn}\}$ also must be selected. The only requirements imposed on $\{\psi_{mn}\}$ are that they are kinematically admissible and complete. If $X_m(x/a)$ and $Y_n(y/b)$ are the normalized beam shape functions satisfying the same static and kinematic boundary conditions as the original laminate, then the functions

$$\psi_{mn}(x, y) = X_m(x/a)Y_n(y/b) \tag{38}$$

are a suitable basis for the laminate.

Now substitution of Eqs. (35–38) into Eq. (5) yields

$$(a^4/ab)K_{pqmn} = D_{11}\mu_p^4\delta_{pm}\,\delta_{qn} + 2D_kC_{pm}c_{nq}R^2$$
$$+ 2D_{16}(H_{pm}g_{nq} + H_{mp}g_{qn})R + D_{22}\nu_q^4\delta_{pm}\delta_{qn}R^4$$
$$+ 2D_{26}(G_{pm}h_{nq} + G_{mp}h_{qn})R^3$$
$$(a^2/ab)M_{pqmn} = C_{mp}\delta_{nq} + \beta R^2\delta_{mp}c_{nq} \tag{39}$$

where $D_k = D_{12} + 2D_{66}$, and

$$\begin{aligned} \mu_p^4\delta_{mp} &= (X_p'', X_m'') & \nu_q^4\delta_{nq} &= (Y_q'', Y_n'') \\ \delta_{pm} &= (X_p, X_m) & \delta_{qn} &= (Y_q, Y_n) \\ C_{pm} &= (X_p'', X_m) & c_{qn} &= (Y_q'', Y_n) \\ G_{pm} &= (X_p', X_m) & g_{qn} &= (Y_q', Y_n) \\ H_{pm} &= (X_p'', X_m') & h_{qn} &= (Y_q'', Y_n') \end{aligned} \tag{40}$$

In Eq. (40), $()'$ indicates differentiation with respect to the indicated argument, $(\cdot,\cdot)$ now denotes the L_2 inner product on (0,1) and μ_p and ν_q are the natural frequencies corresponding to the beam shape functions X_p and Y_q, respectively. The matrix elements (40) are completely determined from the laminate boundary conditions and, consequently, will be called boundary conditions parameters. Substitution of Eq. (39) into Eq. (24) yields the approximation

$$a^2\lambda_{mn} = \frac{\left[D_{11}\mu_m^4 + 2D_kC_{mm}c_{nn}R^2 + D_{22}\nu_n^4R^4\right]}{\left[C_{mm} + \beta R^2 c_{nn}\right]}$$
$$- \frac{1}{\left(C_{mm} + \beta R^2c_{nn}\right)^2}\sum_{p\neq m}^{N}\sum_{q\neq n}^{N}\left[\left\{D_{11}\mu_m^4 + 2D_kC_{mm}c_{nn}R^2\right.\right.$$
$$\left.+ D_{22}\nu_n^4R^4\right\}\left\{C_{mp}\delta_{nq} + \beta R^2\delta_{mp}c_{nq}\right\} - \left\{2D_kC_{pm}c_{nq}R^2\right.$$
$$\left.+ 2D_{16}(H_{pm}g_{nq} + H_{mp}g_{qn})R + 2D_{26}(G_{pm}h_{nq} + G_{mp}h_{qn})R^3\right\}$$
$$\times \left(C_{mm} + \beta R^2c_{nn}\right)\Big]^2 \times \left[\left(C_{mm} + \beta R^2c_{nn}\right)\right.$$
$$\times \left(D_{11}\mu_p^4 + 2D_kC_{pp}c_{qq}R^2 + D_{22}\nu_q^4R^4\right) - \left(C_{pp} + \beta R^2c_{qq}\right)$$
$$\times \left(D_{11}\mu_m^4 + 2D_kC_{mm}c_{nn}R^2 + D_{22}\nu_n^4R^4\right)\Big]^{-1} \tag{41}$$

Equation (41), like Eq. (24), contains only quadratic terms in D_{16} and D_{26}. The order of the truncated terms are $(D_k/D_{11})^3$ and (D_3/D_{11}^3) where D_3 is a cubic polynomial in D_{16} and D_{26}.

Discussion

To provide insight into the development of the approximate closed-form expression for the eigenvalues, it is useful to consider the following illustrative example. Consider a simply supported, four-ply square laminate $[45/-45\,\mathrm{deg}]_s$ loaded under equal biaxial compression. This laminate exhibits the largest twist bending coupling terms D_{16} and D_{26}. The material considered will be a high-modulus ratio graphite-epoxy whose specific material data are given in the next section. Here, attention is focused strictly on the $[K]$ and $[M]$ matrices where, for simplicity, $N = 3$. This simple illustration exhibits all of the essential features encountered in more general problems with much greater degrees of freedom.

To facilitate comparison between approximate and exact (i.e., Ritz) solutions, it is convenient to introduce the following nondimension eigenvalues:

$$k_{mn} = -\left(\lambda_{mn}a^2/U_1t^3\right) \tag{42}$$

All laminates are 4-ply symmetric angle-ply square laminates $[\theta/-\theta]_s$. The Ritz solutions $\hat{k}_m$ are similarly the nondimensionalized buckling loads. Although, the indices m and n in Eq. (41) identify particular eigenvalues, it is not possible to ascertain, a priori, to which approximate eigenvalue the mth Ritz solution corresponds. Thus, when computing approximate buckling loads from these equations, it is necessary to evaluate the eigenvalues for several indices since there is no guarantee which values of m and n produce the lowest approximate eigenvalue. In general, the lowest eigenvalue will occur when either $m = 1$ or $n = 1$, but not necessarily when $m = n = 1$.

Figures 1a and 1b display graphically all of the eigenvalues, exact and approximate. Here $\hat{k}_1, \ldots, \hat{k}_9$ are the nine exact nondimensional eigenvalues, plotted as a function of S, where $0 \le S \le 1$, and $\hat{k}_{ij}$ are the normalized eigenvalues determined from Eq. (41). Since $[M]$ is diagonal, S_2 does not appear, and S_1 has been set equal to S. The Ritz solution is developed by multiplying all off-diagonal elements of $[K]$ by S. The eigenvalues are ordered at $S = 0$, so that

$$\hat{k}_1(0) \le \hat{k}_2(0) \le \cdots \le \hat{k}_9(0) \tag{43}$$

Each $\hat{k}_i(S)$ is chosen to be smooth. Hence, the inequalities (43) may be violated and, indeed, are for a few cases near $S = 1$. Note that $\hat{k}_i(1)$ are the exact eigenvalues of the nine-degrees-of-freedom system that Eq. (41) is attempting to predict.

As observed in Fig. 1a, $\hat{k}_1(S)$ is the lowest eigenvalue for all S. Its approximation, $\hat{k}_{11}(S)$, satisfies $\hat{k}_{11}(0) = \hat{k}_1(0)$, $\mathrm{d}\hat{k}_{11}/\mathrm{d}S = \mathrm{d}\hat{k}_1/\mathrm{d}S = 0$ at $S = 0$, and $\mathrm{d}^2\hat{k}_{11}/\mathrm{d}S^2 = \mathrm{d}^2\hat{k}_1/\mathrm{d}S^2$ at $S = 0$. Using these data, $\hat{k}_1(S)$ may be approximated by a unique parabola. At $S = 1$, the solution $\hat{k}_{11}(1)$ differs from $\hat{k}_1(1)$ by 6.7% for graphite epoxy. The percent difference drops to 3.1% if a smaller modulus material, boron epoxy, is used.

The next pair of curves $\hat{k}_2$ and $\hat{k}_3$ is coincident at $S = 0$. It can be shown that if S is extended to negative values, each of the Ritz solutions is an even function of S. Consequently, this pair of curves has corners at $S = 0$ and neither one is differentiable there. Approximate solutions $\hat{k}_{12}$ and $\hat{k}_{21}$ do not exist. The formula (41) correctly predicts an infinite second derivative at $S = 0$, but otherwise is meaningless.

The next pair, $\hat{k}_4$ and $\hat{k}_5$, is also repeated at $S = 0$. By extending these curves to $S \prec 0$, it can be easily verified that $\hat{k}_4$ has a corner at $S = 0$, but $\hat{k}_5$ is constant and independent of S. An examination of the matrices at $S = 0$ shows that $K_{1331} = K_{3113} = 0$, and $\hat{k}_{13}(0) = \hat{k}_{31}(0) = \hat{k}_4(0) = \hat{k}_5(0)$. Consequently, the second derivative, according to Eq. (41), is the indeterminate form 0/0, consistent with the second derivatives of $\hat{k}_4$ and $\hat{k}_5$ at $S = 0$.

The exact solution $\hat{k}_6(S)$ and its poor approximation $\hat{k}_{22}(S)$ can be clearly observed. Here, $\hat{k}_{22}$ matches $\hat{k}_6$ in value, slope, and second derivativeat $S = 0$. However the second derivative, although

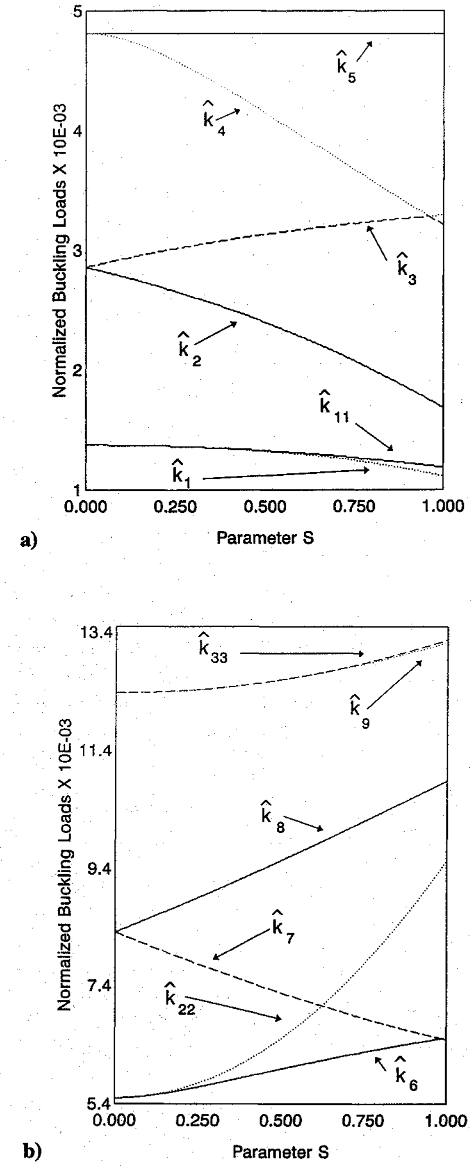

Fig. 1 **Comparison of exact and approximate buckling loads as a function of S for simply supported, square, high stiffness ratio laminate, $N = 3$, $\beta = 1$, and $\theta = 45$ deg.**

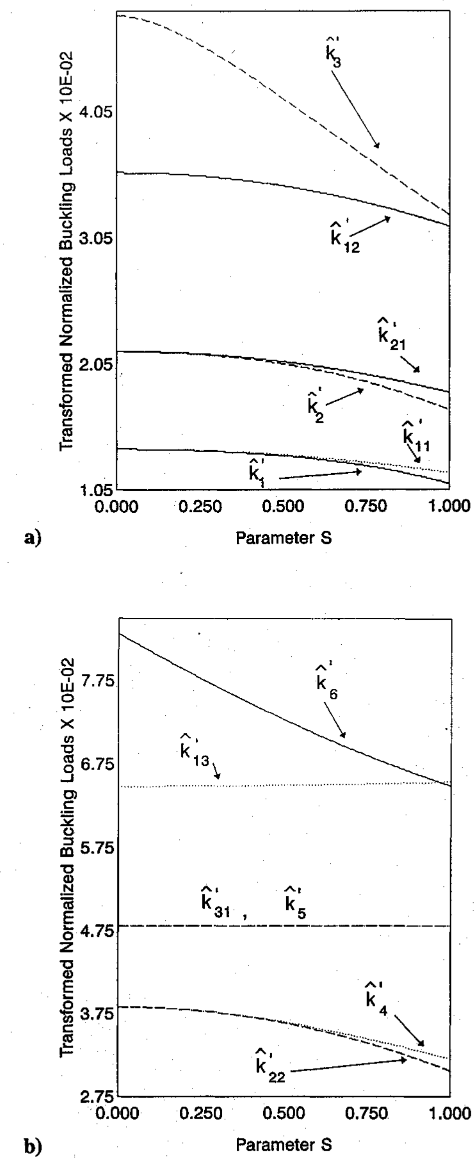

Fig. 2 **Transformed data of Fig. 1; transformation occurs at $k_{12}(0) = k_{21}(0)$ at $\theta = 45$ deg; $k_{31}(0) = k_{22}(0)$ at $\theta = 41$ deg.**

correctly predicted by Eq. (23), is very large because $\hat{k}_{31}(0)$ is close to $\hat{k}_{22}(0)$. The Ritz curve $\hat{k}_6(S)$ and its approximation show almost a 50% disparity at $S = 1$.

The pair $\hat{k}_7$ and $\hat{k}_8$ exhibit the same behavior as $\hat{k}_2$ and $\hat{k}_3$ and, hence, remarks made for the latter pair also apply here. And finally, the curves $\hat{k}_9$ and $\hat{k}_{33}$ coincide virtually throughout the entire range of S.

To obtain curves for the repeated eigenvalues and $\hat{k}_6$ that can be approximated by Eq. (41), it is necessary to apply similarity transformations. These transformations will change (separate) the initial values ($S = 0$) as well as the shape of the Ritz curves. But they will not affect the terminal values, i.e., the desired eigenvalues.

Results for two similarity transformations are shown in Figs. 2a and 2b for the first six eigenvalues. Here the prime denotes eigenvalues obtained from the transformed matrices. Two transformations are employed. One separates the initial values of $\hat{k}_2$ and $\hat{k}_3$. Note that the new curves $\hat{k}'_2$ and $\hat{k}'_3$ attain the same values as $\hat{k}_2$ and $\hat{k}_3$ at $S = 1$, and now meaningful curves $\hat{k}'_{21}$ and $\hat{k}'_{12}$ nicely approximate $\hat{k}'_2$ and $\hat{k}'_3$, respectively. The other transformation employed affects the curves $\hat{k}_1$, $\hat{k}_4$, $\hat{k}_5$, and $\hat{k}_6$. Recall that the off-diagonal elements K_{1331} and K_{3113} vanish and, thus, the transformation (28) reduces to $[Q] = [1]$, whence $[K'] = [K]$. Also, recall that the reason $\hat{k}_{22}(1)$ is a poor estimate of $\hat{k}_6(1)$ is the relative proximity of $\hat{k}_6(0)$ to $\hat{k}_4(0)$.

Indeed, calculations for the four ply symmetric angle-ply laminate with $\theta = 41$ deg, reveals that $\hat{k}_{22}(0) = \hat{k}_{31}(0)$. Consequently, it is convenient to define $[Q]$ as the transformation that separates $\hat{k}_{22}$ and $\hat{k}_{31}$ at $\theta = 41$ deg. With this transformation, $\hat{k}'_4$, $\hat{k}'_5$, and $\hat{k}'_6$ are now well separated at $S = 0$ as shown in Fig. 2. The solution $\hat{k}'_{31}(1)$ is exactly $\hat{k}'_5(1)$, whereas $\hat{k}'_4(1)$ and $\hat{k}'_6(1)$ are reasonably approximated by $\hat{k}'_{22}(1)$ and $\hat{k}'_{13}(1)$, respectively.

The accuracy of the various approximate expressions will be assessed for two different materials. These material are high-modulus graphite epoxy and medium-modulus boron epoxy. The specific moduli E_{11}/E_{22}, E_{11}/G_{12}, and ν_{12} are 40.0, 80.0, and 0.30 for graphite epoxy and 10.0, 40.0, and 0.25 for boron epoxy.

Figures 3 and 4 ($\beta = 1$) depict results for the supported graphite-epoxy and boron-epoxy laminates, respectively. The normalized Ritz solution k_m are obtained by numerically solving Eq. (6). In Fig. 3, it is seen that for $\theta \prec 19$ deg $k_{12} \cong k_1$ and for the central region $k_{11} \cong k_1$. The maximum error occurs at 45 deg and is 5%. Figure 4, however, shows that $k_{11} \cong k_1$ everywhere, and the maximum difference is less than 2%. In Fig. 5, the data are transformed at $\theta = 45$ deg, using the repeated values $\hat{k}_{12}(0) = \hat{k}_{21}(0)$. Here, the second mode k_2 is approximated by k'_{12} for $20 \prec \theta \prec 70$ deg. For $\theta \prec 20$ deg and $\theta \succ 70$ deg, k_2 is accurately approximated by k_{31} and k_{13} (not shown), respectively.

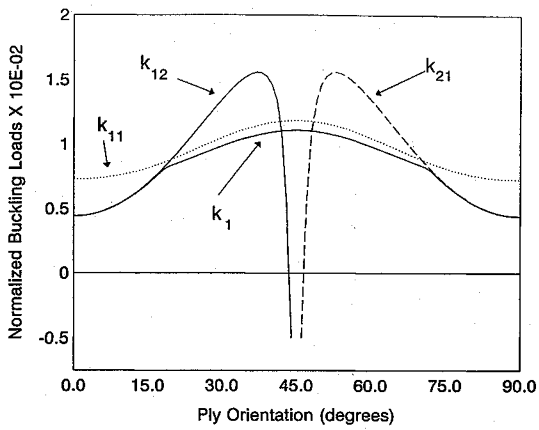

Fig. 3 Effect of ply orientation on normalized buckling loads for a square, simply supported plate using graphite epoxy under biaxial compression $\beta = 1$.

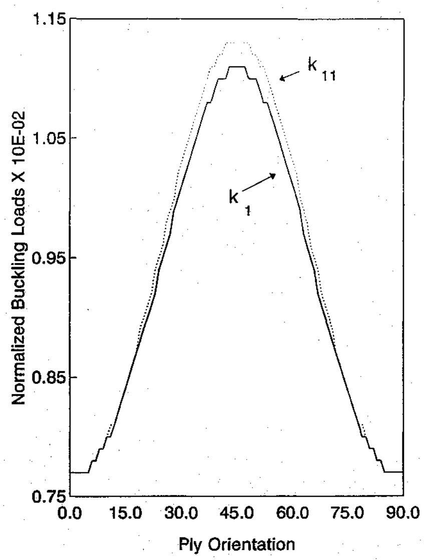

Fig. 4 Effect of ply orientation on normalized buckling loads for a square, simply supported plate using boron epoxy under biaxial compression $\beta = 1$.

Generally, if only the lowest eigenvalue is required, it is not necessary to transform the matrices. Consequently, the curves shown in the remaining figures are all calculated from Eq. (41). Figure 6 shows results for a simply supported graphite-epoxy laminate under uniaxial compression. The eigenvalue k_{21} has a very large slope for $\theta \approx 19$ deg. Here Eq. (41) does not apply, since this eigenvalue $\hat{k}_{21}(0)$ is repeated. Similar remarks apply to $\hat{k}_{31}(0)$ near 27 deg. On the other hand, k_{11} is well behaved throughout the range of angles θ. The maximum deviation of the smallest k_{ij} from the Ritz solution k_1 is 6%, which occurs near $\theta = 53$ deg. In Fig. 7 only the material stiffness ratio has been changed. Here a boron-epoxy material is used. As the ratio E_{11}/E_{22} decreases from 40 to 10, the maximum difference between Eq. (41) and the Ritz solution decreases and is now less than 3%.

Figure 8 shows results for a boron-epoxy laminate simply supported on one pair of opposite edges and clamped on the other. In Fig. 9, three sides of the graphite-epoxy laminated are supported and the remaining side is clamped. Clearly, the results predicted by Eq. (41) are extremely close to the exact buckling loads for both plates.

Finally, the last two figures depict various buckling loads for a square clamped boron-epoxy laminate. For uniaxial compression (Fig. 10) the solution for k_1 is evidently k_{11} for $\theta \prec 48$ deg and k_{21} otherwise. For biaxial compression (Fig. 11) the smallest eigenvalue is k_{12} for $\theta \prec 27$ deg, k_{21} for $\theta \succ 63$ deg, and k_{11} otherwise.

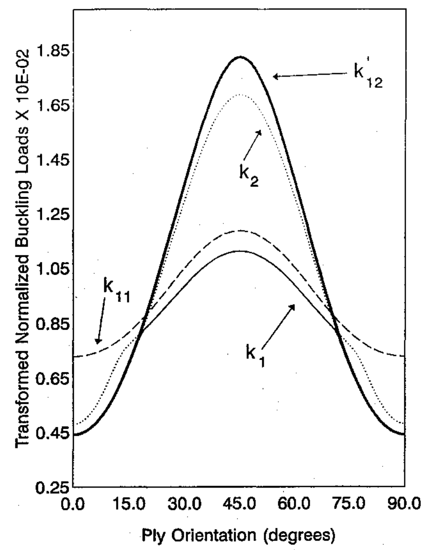

Fig. 5 Effect of ply orientation on transformed buckling loads for the laminate of Fig. 3; transformed data occur at $k_{12}(0) = k_{21}(0)$ at $\theta = 45$ deg.

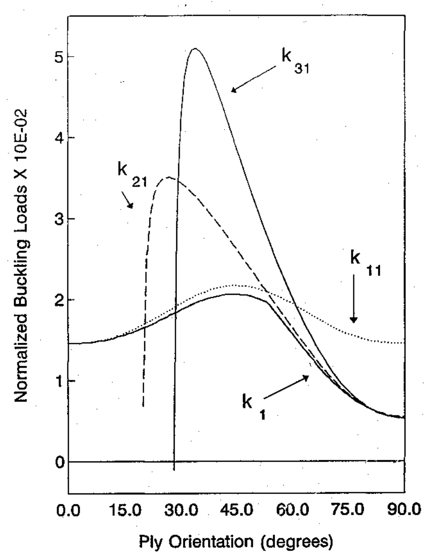

Fig. 6 Effect of ply orientation on normalized buckling loads for a square, simply supported plate using graphite epoxy under unaxial compression $\beta = 0$.

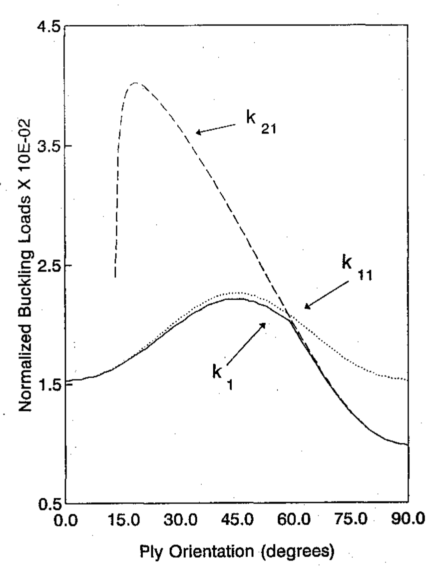

Fig. 7 Effect of ply orientation on normalized buckling loads for a square, simply supported plate using boron epoxy under uniaxial compression $\beta = 0$.

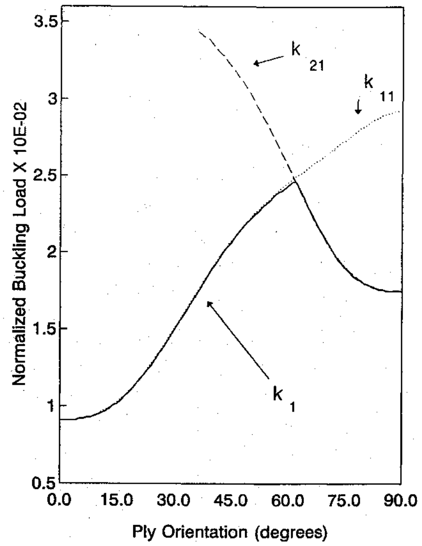

Fig. 8 Effect of ply orientation for a square plate, simply supported on $x = 0, a$ and clamped on $y = 0, b$ for boron epoxy under biaxial compression $\beta = 1$.

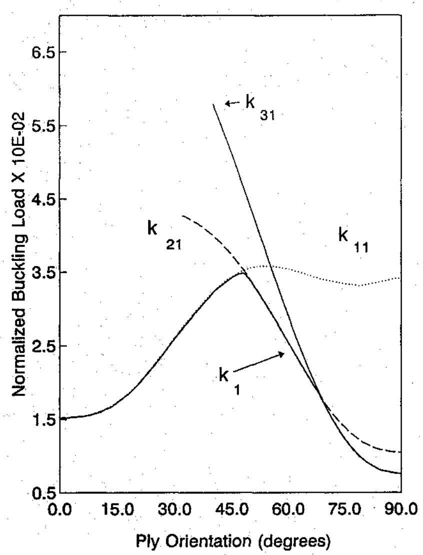

Fig. 9 Effect of ply orientation for a square plate, simply supported on $x = 0, a$ and supported clamped on $y = 0, b$ for graphite epoxy under unaxial compression $\beta = 0$.

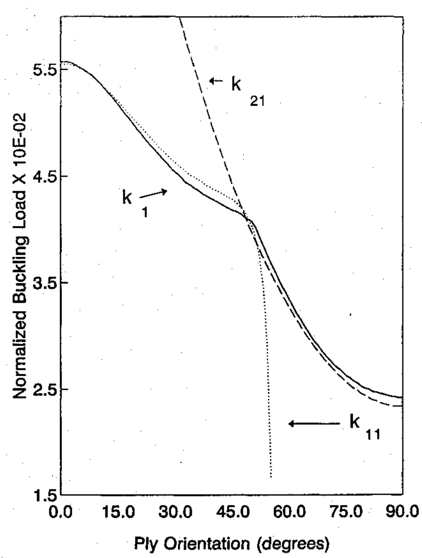

Fig. 10 Effect of ply orientation on normalized buckling loads for a square, clamped plate using boron epoxy under uniaxial compression $\beta = 0$.

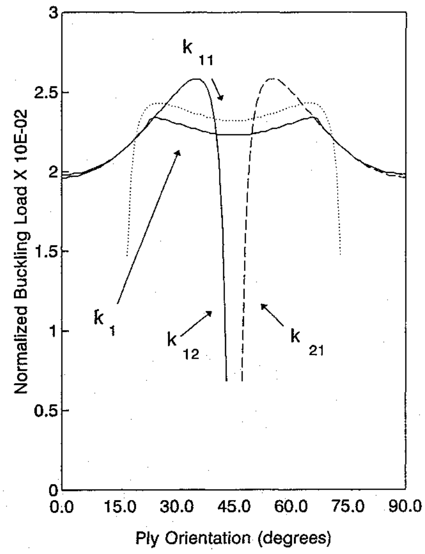

Fig. 11 Effect of ply orientation on normalized buckling loads for a square, simply supported plate using boron epoxy under biaxial compression $\beta = 1$.

Conclusion

An approximation expression has been derived that was used to compute the critical buckling loads for symmetric rectangular angle-ply laminates. The approximate solution (41) was derived from the general results (24) specifically for beam shape functions chosen as basis functions. The accuracy of Eq. (24), which was truncated after quadratic terms, is extremely dependent upon the basis set selected. Although higher order terms could have been included, it would have been at the expense of compromising the simplicity of the result. It has been shown that by using beam shape functions as basis function, for combination of clamped and simply supported boundary conditions, the specialized, Eq. (41) can provide a good, if not excellent, engineering approximation to the critical buckling and higher order buckling load for symmetric rectangular angle-ply laminates. For other boundary conditions or laminate, other choices for the basis functions will be necessary. When the basis functions are properly selected, the advantage of this method over competing computationally based methods is apparent. Whereas the latter approaches require rapidly increasing computational effort as the number of degrees of freedom increases, the present method can handle a very large number of degrees of freedom with relative ease.

Acknowledgments

This study was supported by the Air Force Office of Scientific Research through Contract FC49620-89-C-0003, by NASA through Grant NAG-1445, and by Howard University through a terminal fellowship (Barton).

References

[1]Chamis, C. C., "Buckling of Anisotropic Composite Plates," *Journal of Structural Engineering*, Vol. 10, Oct. 1969, pp. 2119–2139.

[2]Ashton, J. E., and Whitney, J. M., *Theory of Laminated Plates*, Technomic, Westport, CT, 1970, pp. 95–98.

[3]Tauchert, T. R., "Thermal Buckling of Thick Anti-symmetric Angle-Ply Laminates," *Journal of Thermal Stresses*, Vol. 10, No. 2, 1987, pp. 113–124.

[4]Pandey, M., and Sherbourne, A., "Buckling of Anisotropic Composite Plates Under Stress Gradients," *Journal of Engineering Mechanics*, Vol. 117, No. 2, 1991, pp. 260–275.

[5]Tang, W. T., and Sridharan, S., "Buckling Analysis of Anisotropic Plates Using Perturbation Techniques," *Journal of Engineering Mechanics*, Vol. 116, No. 10, 1990, pp. 2206–2222.

[6]Chang, J. C., and Chiu, N. C., "Thermal Buckling Analysis of Antisymmetric Laminated Cylindrical Shell Panels," *International Journal of Solids and Structures*, Vol. 27, No. 10, 1991, pp. 1298–1309.

[7]Lin, C. C., and Kuo, C. S., "Buckling of Laminated Plates with Holes," *Journal of Composite Materials*, Vol. 23, No. 6, 1989, pp. 536–553.

[8]Teply, J. L., Barbero, E. J., and Reddy, J. N., "Bending, Vibration and Stability of ARALL Laminates Using a Generalized Plate Theory," *International Journal of Solids and Structures*, Vol. 27, No. 5, 1991, pp. 585–599.

[9]Chen, W. H., and Yang, S. H., "Buckling Analysis for General Composite Laminates by Hybrid-Stress Finite Element Method," *AIAA Journal*, Vol. 29, No. 1, 1991, pp. 140–147.

[10]Khdeir, A. A., "Free Vibration and Buckling of Symmetric Cross-Ply Laminated Plates by an Exact Method," *Journal of Sound and Vibration*, Vol. 126, No. 3, 1988, pp. 447–461.

[11]Jones, R. M., *Mechanics of Composite Materials*, Scripta , Washington, DC, 1975, pp. 259–267.

[12]Jones, R. M., "Buckling and Vibration of Rectangular Unsymmetrically Laminated Cross-Ply Plates," *AIAA Journal*, Vol. 11, No. 12, 1973, pp. 1626–1632.

[13]Whitney, J. M., "Bending Extension Coupling in Laminated Plates Under Transverse Loading," *Journal of Composite Materials*, Vol. 3, Jan. 1969, pp. 20–28.

[14]Reiss, R., and Barton, O., "On Approximate Closed Form Solutions for Buckling of Anisotropic Rectangular Plates," *Proceedings of the Twenty-First Midwestern Mechanics Conference*, Univ. of Missouri, Abstract, 1991, pp. 48, 49.

[15]Hildebrand, F. B., *Methods of Applied Mathematics*, Prentice–Hall, Englewood Cliffs, NJ, 1965, pp. 1–93.

[16]Reiss, R. "Design Derivatives of Eigenvalues and Eigenvectors of Self-Adjoint Distributed Parameters Systems," *AIAA Journal*, Vol. 24, No. 7, 1986, pp. 1169–1172.